

000 001 002 003 004 005 006 007 008 009 010 011 012 013 014 015 016 017 018 019 020 021 022 023 024 025 026 027 028 029 030 031 032 033 034 035 036 037 038 039 040 041 042 043 044 045 046 047 048 049 050 051 052 053 CONTROLLABLE TEST-TIME SCALING VIA SPARSE AUTOENCODER-BASED REASONING STEERING

Anonymous authors

Paper under double-blind review

ABSTRACT

A common Test-Time Scaling (TTS) strategy for Large Language Models (LLMs) reasoning is allocating additional computation during inference to generate longer Chains-of-Thoughts (CoTs). However, simply scaling CoT length often introduces redundancy and aimless exploration, which can paradoxically degrade performance. We propose that effective TTS requires a shift from merely lengthening reasoning to actively steering reasoning trajectory, thereby directing additional computation toward productive reasoning. To this end, we propose SAE-Scaling, a framework for fine-grained control over an LLM’s reasoning trajectory. SAE-Scaling first employs Sparse Autoencoders to identify and disentangle interpretable features associated with five key reasoning strategies: *Problem Understanding*, *Procedural Planning*, *Backtracking*, *Multi-perspective Verification*, and *Hypothesis Reasoning*. Next, we train a lightweight strategy router that dynamically chooses a reasoning strategy at each step of the reasoning trajectory. By actively manipulating the strategy-specific feature during generation, SAE-Scaling steers the CoT to follow a target reasoning strategy, thereby channeling the additional computation to more productive reasoning. Experiments on three LLMs across three challenging reasoning benchmarks show a 68% average success rate in controlling reasoning strategies alongside an average absolute accuracy gain of 3.6% over the vanilla baseline, highlighting the effectiveness of SAE-Scaling.

1 INTRODUCTION

Test-Time Scaling (TTS) has emerged as a promising direction in improving Large Language Models (LLMs) on complex reasoning tasks such as mathematical problem solving and code generation (Jaech et al., 2024; OpenAI, 2025; Guo et al., 2025). An effective strategy of TTS is to allocate additional computation for producing longer Chains of Thought (CoTs) (Wei et al., 2022), as evidenced by the success of GPT-o3 (OpenAI, 2025) and DeepSeek-R1 (Guo et al., 2025). These long CoTs incorporate human-like reasoning strategies such as verification and backtracking (Gandhi et al., 2025; Marjanović et al., 2025; Pan et al., 2025; Kumar et al., 2025), which significantly improve both the accuracy and the robustness of LLMs (Snell et al., 2025; Zaremba et al., 2025; Muennighoff et al., 2025).

To extend CoTs for TTS while avoiding expensive training, recent studies have been exploring training-free strategies. Several popular approaches scale the CoT length by inserting special tokens (*e.g.*, `wait`) late in the reasoning process (Muennighoff et al., 2025). Alternative methods identify and manipulate length-related control vectors within the hidden-state space of LLMs to generate longer CoTs (Sun et al., 2025; Tang et al., 2025; Chen et al., 2025). However, these extended CoTs often contain repetitive arguments or aimless explorations, undermining the overall effectiveness of TTS (Zeng et al., 2025; Gema et al., 2025). This issue stems from extended CoTs adopting erroneous reasoning strategies. As illustrated in Figure 1a, when the reasoning path contradicts the original question, repeated calculation verification offers no remedy. Instead, LLM should be steered to re-understand the problem itself.

To address this issue, we formalize a new task: *reasoning steering* for controllable TTS. Instead of blindly extending CoTs, this task aims to actively steer the LLM’s reasoning process by controlling the underlying reasoning strategies. A critical challenge in this task is to steer the LLM to follow a pre-specified reasoning strategy. Existing vector-steering methods (Sun et al., 2025; Sheng et al.,

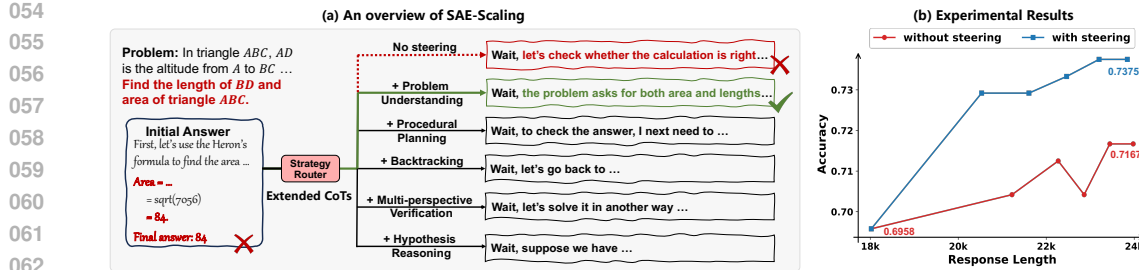


Figure 1: (a) Overview of SAE-Scaling. During inference, the strategy router identifies an effective reasoning strategy for the given context and steers the extended CoT towards this strategy by manipulating SAE features, yielding a more productive reasoning trajectory. (b) Performance of Qwen3-8B on AIME25. By steering the reasoning strategy, we achieve better performance under the same amount of additional test-time computation.

2025), however, are inadequate for this purpose. Their control vectors primarily affect CoT length without aligning with discrete reasoning strategies (see detailed analysis in Section 2).

To overcome this, we propose leveraging Sparse Autoencoders (SAEs) (Huben et al., 2024) to decompose the LLM’s hidden states into a sparse set of interpretable and monosemantic features (Bricken et al., 2023). Specifically, a well-trained SAE will project the low-dimensional, strategy-entangled hidden states of an LLM into a high-dimensional, disentangled feature space. This projection aims to isolate strategy-specific features in the high-dimensional space, thereby providing disentangled control vectors for reasoning strategy steering.

In this light, we propose SAE-Scaling, a controllable TTS framework to steer LLMs’ reasoning to follow effective reasoning strategies. SAE-Scaling first trains an SAE to decompose the LLM’s hidden states into a large set of disentangled features via sparsity and reconstruction constraints. It then applies a multi-stage pipeline to identify strategy-specific features from the large set of SAE features. This pipeline progressively filters features using correlation logits, causal effect, and task accuracy, balancing identification efficiency with accuracy. By treating these strategy-specific features as control vectors and shifting the hidden states of LLMs during decoding, we can steer the LLM to follow the corresponding reasoning strategy. Moreover, to avoid manual intervention on strategy selection, SAE-Scaling trains a lightweight strategy router via contrastive learning (van den Oord et al., 2018). This router assesses the ongoing reasoning context to dynamically select an effective strategy for subsequent generation.

We conduct extensive experiments on three LLMs of varying scales over three challenging mathematical reasoning benchmarks. The results show that SAE-Scaling achieves an average of 68% success rate in reasoning strategy control, alongside an average absolute accuracy improvement of 3.6% over the vanilla baseline, underscoring the effectiveness of SAE-Scaling.

In summary, our contributions are threefold: (1) We pioneer the task of explicit reasoning strategy control for CoT generation, and propose SAE-Scaling to disentangle and identify strategy-specific features for reasoning steering. (2) We propose a multi-stage pipeline to progressively identify strategy-specific features, addressing the challenge of efficient feature selection from the massive set of SAE features. (3) Extensive experiments validate the effectiveness and rationality of the proposed SAE-Scaling framework, showing the significant potential of controlling LLMs’ reasoning trajectory for TTS.

2 PRELIMINARY

Reasoning Steering. We formulate the task of *reasoning steering*, which aims to control LLMs’ reasoning strategy by directly manipulating their internal states. In a standard autoregressive setting, an LLM generates the next token y_t based on the prefix $Y_{<t} = \{y_1, \dots, y_{t-1}\}$. The LLM processes $Y_{<t}$ through its L transformer layers, producing a sequence of residual stream activations $\{\mathbf{x}_t^1, \mathbf{x}_t^2, \dots, \mathbf{x}_t^L\}$. In vanilla decoding, these activations remain unmodified. Reasoning steering

108 departs from this by injecting a control vector $\Delta \mathbf{x}^i$ at a specific layer i :

$$109 \quad \mathbf{x}'^i_t = \mathbf{x}_t^i + \alpha \cdot \Delta \mathbf{x}^i, \quad (1)$$

110 where $\alpha \in \mathbb{R}$ is a coefficient controlling the steering strength. The activation \mathbf{x}'^i_t then
 111 replaces \mathbf{x}_t^i and is propagated through the remaining layers, influencing the final generation. By
 112 repeating this intervention for N consecutive tokens, the LLM produce a steered trajectory $Y' =$
 113 $\{y'_t, y'_{t+1}, \dots, y'_{t+N-1}\}$. Given a pre-specified reasoning strategy s , the goal of reasoning steering
 114 is to construct $\Delta \mathbf{x}^i$ that ensures the steered trajectory Y' aligns with s .

115
 116 **Conceptual Entanglement of Vector Steering.** Previous methods typically derive control vectors by contrasting activations from disparate reasoning behaviors (Tang et al., 2025; Chen et al., 2025; Zhu et al., 2025). For example, they compute the activation difference between long and short
 117 CoT trajectories to obtain a vector that modulates reasoning strength (Sun et al., 2025). However, a key limitation of such control vectors is conceptual entanglement (Elhage et al., 2022;
 118 Yang et al., 2025b). They often conflate multiple reasoning strategies, rendering them inseparable.
 119 Consequently, their manipulation yields only coarse-grained effects, such as altering reasoning
 120 length (Sheng et al., 2025), but lacks the precision required to steer the LLM towards a specific
 121 reasoning strategy. To overcome this limitation, we leverage SAEs to decompose LLM activations
 122 into a basis of disentangled and interpretable features (Bricken et al., 2023), enabling fine-grained
 123 strategic control.

124 3 METHOD

125 Due to limited space, we refer to Appendix C for Related Work. In this section, we present SAE-
 126 Scaling, a controllable TTS framework that steers LLMs’ reasoning trajectory by controlling its
 127 reasoning strategy. We first describe how we steer the reasoning strategies by manipulating strategy-
 128 specific features identified in the SAE (Section 3.1), and outline the pipeline used to discover these
 129 features (Section 3.2). We then introduce a strategy router that dynamically chooses the effective
 130 reasoning strategy for a given reasoning context (Section 3.3).

131 3.1 REASONING STEERING WITH DISENTANGLED SAE FEATURES

132 We train SAEs to disentangle and identify strategy-specific features, which then serve as the control
 133 vectors for reasoning steering. As illustrated in Figure 2a, an SAE is an encoder–decoder archi-
 134 tecture trained to represent an input activation as a sparse linear combination of learned feature
 135 directions. Given a residual stream activation $\mathbf{x} \in \mathbb{R}^N$, it encodes \mathbf{x} into a sparse feature activation
 136 vector $\mathbf{s} \in \mathbb{R}^M$ ($M \gg N$) and reconstructs it as $\hat{\mathbf{x}}$:

$$137 \quad \mathbf{s} = \sigma(\mathbf{W}_{\text{enc}}(\mathbf{x} - \mathbf{b}_{\text{dec}}) + \mathbf{b}_{\text{enc}}), \quad (2)$$

$$138 \quad \hat{\mathbf{x}} = \mathbf{W}_{\text{dec}}\mathbf{s} + \mathbf{b}_{\text{dec}}, \quad (3)$$

139 where $\mathbf{W}_{\text{enc}} \in \mathbb{R}^{N \times M}$, $\mathbf{b}_{\text{enc}} \in \mathbb{R}^M$, $\mathbf{W}_{\text{dec}} \in \mathbb{R}^{M \times N}$, $\mathbf{b}_{\text{dec}} \in \mathbb{R}^N$, and σ is an activation function.

140 The SAE is trained to satisfy a dual objective: (1) minimizing the reconstruction error $\|\mathbf{x} - \hat{\mathbf{x}}\|_2^2$ and
 141 (2) enforcing a sparsity restriction, which dictates that the reconstruction must be constructed from
 142 only a few active latent directions¹. This training process enables the SAE to approximate \mathbf{x} as a
 143 sparse linear combination of the decoder rows:

$$144 \quad \mathbf{x} \approx \mathbf{b}_{\text{dec}} + \sum_{i=1}^M s_i(\mathbf{x}) \mathbf{f}_i \quad (4)$$

145 where each row \mathbf{f}_i of \mathbf{W}_{dec} corresponds to a disentangled and interpretable latent direction, which
 146 we refer to as a *feature* throughout the paper. The coefficients $s_i(\mathbf{x})$ are the i -th component of the
 147 activation vector \mathbf{s} , indicating the activation strength of each feature for the input \mathbf{x} .

148 A key benefit of this decomposition is that the sparsity objective encourages *monosemanticity*
 149 (Bricken et al., 2023): each learned feature tends to capture a single concept, significantly

150
 151 ¹We enforce sparsity via a Top- K activation function, which only retains the K largest activation values
 152 and sets the rest to zero, following Gao et al. (2025).

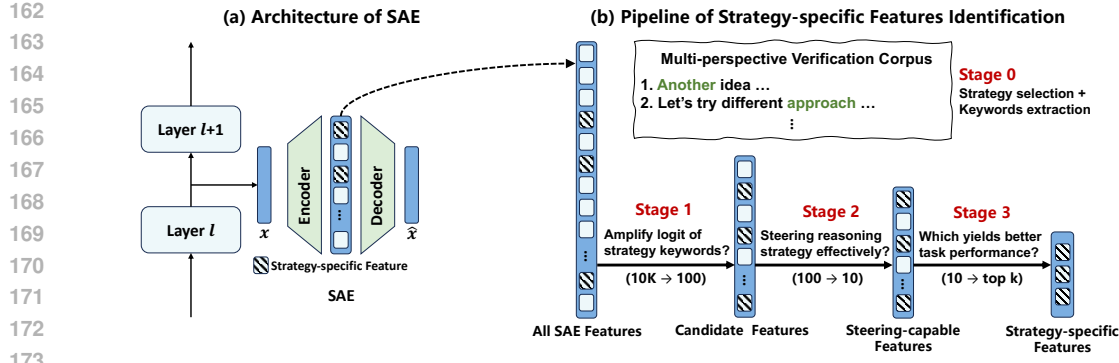


Figure 2: (a) Overview of the SAE architecture. (b) Our strategy-specific feature identification pipeline. Numbers below the arrows indicate the approximate count of features retained, highlighting the orders-of-magnitude reduction at each stage.

mitigating the feature entanglement (Huben et al., 2024). We aim to identify features \mathbf{f}_s that are associated with specific reasoning strategies (see identification methods in Section 3.2). By using \mathbf{f}_s as the control vector $\Delta \mathbf{x}$ in Eq. 1, we steer the LLM’s reasoning strategy by repeatedly injecting \mathbf{f}_s into the residual stream activations at the SAE-trained layer i for the next N generation steps:

$$\mathbf{x}'_{t+k}^i = \mathbf{x}_{t+k}^i + \alpha \cdot \mathbf{f}_s, \quad k = 0, 1, \dots, N-1 \quad (5)$$

where α is the steering strength. The selection of α is a trade-off: excessively large values cause repetitive outputs (Fu et al., 2021), while excessively small values fail to steer effectively. For each feature, we determine α by searching downwards from an empirically chosen high value, iteratively decreasing it until repetitive generation is eliminated (see Appendix D.1 for details).

3.2 IDENTIFICATION OF STRATEGY-SPECIFIC FEATURES

A central challenge in SAE-based reasoning steering is to identify the few critical, strategy-specific features from a vast pool of tens of thousands of candidates. To this end, we propose a three-stage identification pipeline that progressively narrows the feature set using criteria of increasing fidelity and computational cost. As shown in Figure 2b, the process begins with a broad, inexpensive screening based on logit contributions, followed by a more rigorous causal effect ranking stage, and culminates in a final selection based on direct impact on downstream task accuracy.

Stage 0: Strategy Selection and Keyword Extraction. As a preliminary step, we first select a set of reasoning strategies for steering and then extract representative strategy keywords. These keywords serve as a computationally efficient proxy to identify features potentially correlated with a given strategy in Stage 1. As shown in Figure 1, we focus on five reasoning strategies : (1) *Problem Understanding*, where the LLM rephrases the problem statement, clarifying its constraints and interpreting the given information; (2) *Procedural Planning*, where the LLM defines a sub-task or outlines a plan for the subsequent reasoning process; (3) *Backtracking*, where the LLM identifies a mistake in its own previous reasoning and attempts to correct it or revert to a prior step; (4) *Multi-Perspective Verification*, where the LLM attempts to verify its conclusion by applying a different method or examining specific cases; and (5) *Hypothesis Reasoning*, where the LLM makes an assumption or poses a “what if” scenario to explore possibilities or test certain conditions.

While other reasoning strategies may exist, we focus on these five as they are frequent, effective, and widely adopted in prior work (Gandhi et al., 2025; Zhong et al., 2024). For each selected strategy, we extract strategy keywords following the approach of Galichin et al. (2025). Briefly, we first create a strategy-specific corpus by manually identifying reasoning segments in the LLM’s responses. We then extract the most frequent words from each corpus to serve as strategy keywords. Ultimately, this stage identify five distinct reasoning strategies, each associated with a curated set of keywords (see Appendix D.2 for the full list and identification details).

Stage 1: Logit-based Recall. In the first stage, we aim to distill a small set of promising candidates from tens of thousands of SAE features using a low-cost and highly efficient process. This

is accomplished by selecting features that positively influence the logits of strategy keywords. The guiding hypothesis is that features which substantially increase these keyword logits are more likely to steer the LLM toward the corresponding reasoning strategy. We estimate each feature’s direct logit contribution to strategy keywords using logit lens (Nanda & Bloom, 2022; nostalgebraist, 2020), which is highly efficient as it requires only a single matrix multiplication.

Formally, recalling from Section 3.1, the SAE decoder matrix $\mathbf{W}_{\text{dec}} \in \mathbb{R}^{M \times N}$ contains the disentangled feature \mathbf{f}_i as its i -th row. Let $\mathbf{U} \in \mathbb{R}^{N \times V}$ be the LLM’s unembedding matrix, mapping activations to logits over the vocabulary of size V . We calculate the logit contribution of all features simultaneously by calculating the logit contribution matrix $\mathbf{L} \in \mathbb{R}^{M \times V}$:

$$\mathbf{L} = \mathbf{W}_{\text{dec}} \cdot \mathbf{U} \quad (6)$$

where each row $\mathbf{L}_{i,:}$ represents the logit contribution of feature f_i across the entire vocabulary. For each feature, we then examine the top-10 tokens that have the largest positive logit contributions for each feature, and recall the feature if (i) at least n of these tokens are strategy keywords and (ii) each such keyword’s logit contribution exceeds a threshold τ . This recall step is highly selective, narrowing the candidate pool from tens of thousands of features to several hundred.

Stage 2: Causal Effect Ranking. In the second stage, we refine the candidate features from Stage 1 by ranking them based on their causal effect on strategy induction. This enables us to more accurately identify features that are truly effective for steering. We quantify the causal effect as the Average Treatment Effect (ATE) (Rubin, 1974), computed on a small validation set P (e.g., several problem-answer pairs).

Formally, for each problem p and its response prefix $Y_{<t}$ in P , we generate a subsequent N -token trajectory Y' under two distinct conditions. Under the treatment condition ($do(T = 1)$), Y' is generated using reasoning steering with the candidate feature \mathbf{f}_s as control vector, as described in Eq. 5. In contrast, the control condition ($do(T = 0)$) generates Y' via standard autoregressive decoding. Let $R_p \in \{0, 1\}$ be the outcome variable indicating whether Y' aligns with strategy s for problem p ². The ATE of feature \mathbf{f}_s is then estimated as:

$$\text{ATE}(\mathbf{f}_s) = \mathbb{E}_{p \in P} [R_p | do(T = 1)] - \mathbb{E}_{p \in P} [R_p | do(T = 0)] \quad (7)$$

which quantifies the average increase in the probability that the LLM follows strategy s as a direct result of manipulating feature f^3 . A feature is retained if $\text{ATE}(\mathbf{f}_s) \geq \delta$. This process yields a set of approximately ten steering-capable features for each strategy.

Stage 3: Task Accuracy Ranking. The final stage ranks features by their direct impact on task accuracy. This step is necessary because the causal ranking from Stage 2 only confirms a feature’s ability to control the reasoning strategy, not its utility in improving task performance. By filtering for accuracy, we ensure our final feature set is both steering effective and practically useful. To do this, we first collect a set of problems from the validation set that the LLM initially answers incorrectly. For each incorrect answer, we extended its reasoning trajectory by applying reasoning steering, using each steering-capable feature individually as a control vector. We then measure the proportion of these initial errors that are subsequently corrected, which we define as the correction rate. For each of the five target reasoning strategies, we select the Top- k features with the highest correction rates as its final feature set.

3.3 DYNAMIC STRATEGY SELECTION

Reasoning strategies can be controlled either manually or by an automatic strategy router. Here we train a lightweight router via contrastive learning to select the effective strategy based on current reasoning context, thereby obviating the need for manual intervention.

Specifically, we instantiate the strategy router as a bi-encoder architecture (Karpukhin et al., 2020). A context encoder, $E_c(\cdot)$, embeds the current reasoning state (represented by the final token of the

²This alignment can be assessed either by human annotators or by an LLM-as-judge. In Appendix D.4, we discuss the methodology of using LLM-as-judge and validate its reliability against human judgments.

³We set the sampling temperature to 0 when estimating ATE to remove confounding effects from sampling randomness.

270 response prefix $Y_{<t}$), and a feature encoder, $E_f(\cdot)$, projects each strategy-specific feature \mathbf{f}_s into the
 271 same representation space. The effective scores between the context and a feature is then computed
 272 as the dot product of their respective embeddings:

$$273 \quad \text{score}(Y_{<t}, \mathbf{f}_s) = \langle E_c(Y_{<t}), E_f(\mathbf{f}_s) \rangle \quad (8)$$

275 The router is trained using the InfoNCE loss (van den Oord et al., 2018), which encourages higher
 276 effective scores for positive context–feature pairs and lower effective scores for negative ones:

$$277 \quad L(Y_{<t}, \mathbf{f}_s^+, \mathbf{f}_{s,1}^-, \dots, \mathbf{f}_{s,M}^-) = -\log \frac{e^{\text{score}(Y_{<t}, \mathbf{f}_s^+)}}{e^{\text{score}(Y_{<t}, \mathbf{f}_s^+)} + \sum_{k=1}^M e^{\text{score}(Y_{<t}, \mathbf{f}_{s,k}^-)}}, \quad (9)$$

280 where $(Y_{<t}, \mathbf{f}_s^+)$ is labeled as a positive pair if steering with feature \mathbf{f}_s^+ leads to a correct final answer.
 281 All other pairings for that context are treated as negative pairs. At inference time, for a given context
 282 $Y_{<t}$ we compute $\text{score}(Y_{<t}, \mathbf{f}_s)$ for all candidate features \mathbf{f}_s and select the feature with the highest
 283 effective score as the selected features to steer the LLM.

285 4 EXPERIMENTS

288 In this section, we conduct experiments to address the following research questions:

- 290 • **RQ1:** Can our SAE-based reasoning steering method, leveraging the identified features, reliably
 291 steer LLMs’ reasoning strategy?
- 292 • **RQ2:** Can our proposed SAE-Scaling framework improve performance of LLMs on complex
 293 reasoning tasks?
- 294 • **RQ3:** What are the specific contributions of each key component of our framework, and how
 295 sensitive is the overall performance to its critical hyperparameters?

297 4.1 EXPERIMENT SETUP

299 **Datasets and Evaluation Protocol.** Our method is evaluated on three challenging math reasoning
 300 benchmarks: AIME’24, AIME’25 (AIME, 2025), and HMMT (Balunović et al., 2025). A strict
 301 separation is maintained between these test sets and the corpora used for SAE training, feature
 302 identification, and router training (see Appendix D.3 for training corpora details). To evaluate the
 303 steering success rate, we use GPT-4o as an automated judge, whose reliability is confirmed by a high
 304 agreement rate (0.82) with human annotators (see Appendix D.4 for details). To assess reasoning
 305 performance, we report the average accuracy across eight sampled outputs per problem.

306 **Implementation Details.** We implement our framework on three Qwen3 models (8B, 14B, and
 307 32B) (Team, 2025b), training SAEs on the final transformer layer’s residual activations. This layer
 308 is chosen because it is closest to the unembedding layer, which facilitates a more accurate estimation
 309 of feature contributions to the output logits (nostalgebraist, 2020). For sampling, we set the temper-
 310 ature to 0 during steering effectiveness evaluations to eliminate confounding effects from sampling
 311 stochasticity. For other experiments, we adopt the officially recommended temperature of 0.6. For
 312 feature selection, we set the Top- $k=3$ to retain the top three features from candidates, yields a final
 313 of 15 strategy-specific features in total (three per strategy). And we intervene the first 512 generated
 314 tokens for reasoning steering. More implementation details are provided in Appendix D.5.

315 4.2 EFFECTIVENESS OF SAE-BASED REASONING STEERING (RQ1)

317 In this section, we evaluate whether our identified strategy features can achieve fine-grained control
 318 over an LLM’s reasoning strategy. We first conduct quantitative analysis. Specifically, we evaluate
 319 on a randomly sample 100 responses from the AIME dataset. As a comparison baseline, we test
 320 directly boosting the logits of the corresponding strategy-related keywords for controlling strategies.
 321 The results are shown in Table 1, from which we make the following observations:

- 323 (1) SAE-based steering consistently yields high steering success rates (all > 50%), validating our
 324 pipeline’s ability to identify effective strategy-specific features;

324
325
326
327 Table 1: Steering effect of five reasoning strategies evaluated on Qwen3-8B. Keyword denotes
328 keyword-boosting baseline, while SAE denotes our SAE-based reasoning steering.
329

Strategy	Steering Success Rate		BLEU-4		ROUGE-L	
	Keyword	SAE	Keyword	SAE	Keyword	SAE
Problem Understanding	0.14	0.52	0.8695	0.2900	0.8641	0.3044
Procedural Planning	0.72	0.84	0.3823	0.3757	0.3932	0.3604
Backtracking	0.27	0.58	0.5301	0.3486	0.5218	0.3264
Multi-Perspective Verification	0.47	0.79	0.5611	0.3237	0.5569	0.3262
Hypothesis Reasoning	0.45	0.65	0.5586	0.2869	0.5546	0.2988

334
335
336 (2) In contrast, keyword-boosting baseline consistently underperforms SAE-based steering, with
337 success rates dropping as low as 14% for *Problem Understanding* and 27% for *Backtracking*.
338 This suggests our SAE features capture complex strategic patterns beyond simple amplifying
339 the logit of strategy keywords;
340 (3) SAE-steered responses exhibit lower word-level (BLEU-4) and sentence-level (ROUGE-L) sim-
341 ilarities to the unsteered counterparts compared to baselines. This suggests that SAE-based
342 steering produces substantially different outputs, rather than making minor, localized edits.

343 We further present a case study in Figure 3 to illustrate the su-
344 periority of our SAE-based reasoning steering. Without any
345 steering, the LLM attempts to verify its answer by testing dif-
346 ferent values of m . The keyword-boosting baseline proves su-
347 perficial: while it forces the model to generate a target key-
348 word like “another”, it fails to alter the reasoning strategy. In
349 contrast, our SAE-based reasoning steering successfully steer
350 the LLM to a follow *Multi-Perspective Verification* strategy,
351 where the LLM try to approaches the problem in another meth-
352 ods. This case qualitatively corroborates our quantitative find-
353 ings (lower BLEU/ROUGE), confirming that our method in-
354 duces deep, structural changes to the reasoning path, not just
355 superficial edits. Additional examples are available in Figure 7.

356 4.3 OVERALL PERFORMANCE (RQ2)

357 In this section, we evaluate the overall performance of SAE-Scaling. We compare our approach
358 against Budget Forcing (Muennighoff et al., 2025), which extends the reasoning trajectory by ap-
359 pending *wait* tokens. For both methods, we begin with the initial LLM outputs and extend their
360 reasoning trajectories by four additional turns. We then report the accuracy and reasoning length
361 after two and four extension turns. The results, presented in Table 2, reveal three key findings:
362

363 (1) Both Budget Forcing and SAE-Scaling exhibit consistent accuracy improvements as the num-
364 ber of extension turns increases. With four additional extension turns, SAE-Scaling and Budget
365 Forcing achieve average absolute accuracy gains of 3.6% and 2.2%, respectively. This con-
366 firms that allocating additional computation budget and generating longer Chains-of-Thought
367 generally benefits LLM performance (Snell et al., 2025).
368 (2) SAE-Scaling (2 turns) outperforms Budget Forcing (4 turns) on most of datasets, and also
369 achieves a higher average accuracy across all three LLMs. This highlights the importance of
370 selecting effective reasoning strategies during TTS: by steering the LLM towards more effective
371 reasoning strategies, SAE-Scaling generates more productive reasoning trajectories, achieving
372 better accuracy with less additional computation.
373 (3) The largest gains of SAE-Scaling occur within the first two turns, where the reasoning length
374 increases by 20% on average, but accuracy rises by 3.05% in absolute average accuracy. In
375 contrast, the next two turns add an additional 10% to the reasoning length while yielding only a
376 0.55% accuracy gain. This may because that under effective strategy guidance, most correctable
377 reasoning errors are resolved early in the extension process, while later turns mainly address
harder or less recoverable errors, resulting in diminishing returns.

No steering:
Wait, $m=132$ is the first one with four primes. But let me check $m=132$ again. Is there a smaller m ?
Wait, $m=105: 10931=17 \times 643$. Two primes.
...

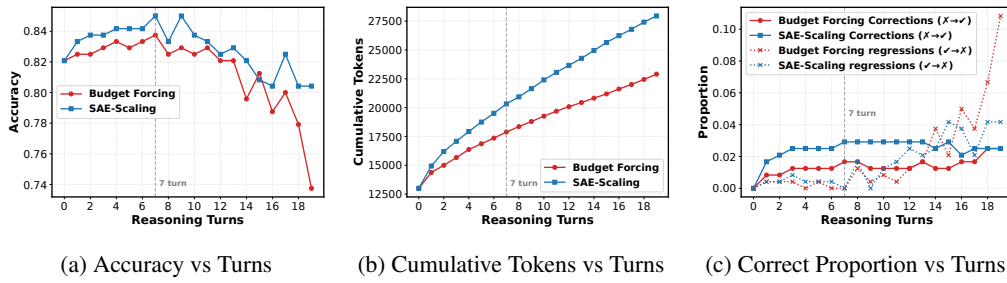
Direct increase logit:
Wait, $m=132$ is the first one with four primes. But let me check $m=another$ value. For example, $m=another$ number where the expression could be composite with more factors.
...

SAE-based reasoning steering:
Alternatively, maybe I can think of another approach. Maybe the original problem is similar to the Euler's prime-generating polynomial but with a different constant term. Maybe the numbers can be factored in another way.
...

Figure 3: Case study of steering.

378
 379 Table 2: Comparison of accuracy (Acc) and reasoning length (Token) on three datasets across three
 380 LLMs. The best results are highlighted in bold, the second-best results are underlined. We extend
 381 the initial answers using Budget Forcing and SAE-Scaling for four extension turns.

382 Model	383 Method	384 AIME24		385 AIME25		386 HMMT		387 Average	
		388 Acc	389 Token	390 Acc	391 Token	392 Acc	393 Token	394 Acc	395 Token
384 Qwen3-8B	Vanilla Baseline	0.7667	14597	0.6958	18024	0.4125	20111	0.6250	17577
	+ Budget Forcing (2 turn)	0.7833	+2994	0.7125	+4249	0.4417	+3707	0.6458	+3650
	+ Budget Forcing (4 turn)	0.7917	+4268	0.7167	+5422	<u>0.4542</u>	+5132	0.6542	+4947
	+ SAE-Scaling (2 turn)	0.7875	+3139	<u>0.7292</u>	+3583	0.4500	+3721	<u>0.6556</u>	+3481
	+ SAE-Scaling (4 turn)	0.7917	+4518	0.7375	+5178	0.4583	+5451	0.6625	+5049
	w/o router (4 turn)	0.7833	+4508	<u>0.7292</u>	+4888	<u>0.4542</u>	+5508	<u>0.6556</u>	+4968
389 Qwen3-14B	Vanilla Baseline	0.7833	13593	0.7333	16416	0.4708	18426	0.6625	16145
	+ Budget Forcing (2 turn)	0.7833	+2325	0.7500	+2615	0.4833	+3337	0.6722	+2759
	+ Budget Forcing (4 turn)	0.7875	+3637	0.7500	+3764	0.4833	+4967	0.6736	+4123
	+ SAE-Scaling (2 turn)	<u>0.7958</u>	+2791	0.7583	+2988	0.5208	+3951	<u>0.6916</u>	+3243
	+ SAE-Scaling (4 turn)	0.8042	+4304	0.7625	+4498	0.5208	+5573	0.6958	+4792
	w/o router (4 turn)	0.7958	+3914	0.7625	+4483	0.5125	+5589	0.6903	+4662
394 Qwen3-32B	Vanilla Baseline	0.8208	13002	0.7500	15766	0.5292	17776	0.7000	15515
	+ Budget Forcing (2 turn)	0.8250	+1994	0.7708	+2686	0.5625	+3096	0.7194	+2592
	+ Budget Forcing (4 turn)	0.8333	+3366	0.7750	+4052	0.5708	+4563	0.7264	+3994
	+ SAE-Scaling (2 turn)	<u>0.8375</u>	+3239	<u>0.7792</u>	+2942	<u>0.5833</u>	+3782	<u>0.7333</u>	+3321
	+ SAE-Scaling (4 turn)	0.8417	+4928	0.7833	+4798	0.5875	+5879	0.7375	+5202
	w/o router (4 turn)	0.8375	+4558	0.7792	+4768	0.5708	+5458	0.7292	+4928



401
 402 Figure 4: Impact of extended reasoning turns on performance. Results are for Qwen3-32B on
 403 AIME24. More results for other LLMs are reported in Appendix Figure 6.

4.4 IN-DEPTH ANALYSIS (RQ3)

413
 414 In this section, we aim to assess the contribution of our strategy router and the sensitivity of SAE-
 415 Scaling to key hyperparameters. First, an ablation study verifies the router’s effectiveness. Second,
 416 we investigate the impact of three hyperparameters on performance: the number of intervention
 417 turns, the number of intervention tokens, and the Top- k feature selection.

418
 419 **Ablation Study.** We assess the strategy router’s contribution by replacing it with a random feature
 420 selection mechanism, denoted as “w/o Router”. The results in Table 2 highlight two findings: (1)
 421 Our router-guided SAE-Scaling (2 turns) matches or surpasses the performance of random selection
 422 (4 turns), achieving higher average accuracy across all LLMs. This demonstrates the router’s ability
 423 to identify effective strategies in early turns. (2) Even the random selection baseline outperforms
 424 the Budget Forcing baseline. We attribute this to our pipeline’s third stage, which ranks all features
 425 based on task accuracy, ensuring their practically useful.

426
 427 **Impact of Extension Turns.** We investigate how the number of extended reasoning turns affects
 428 the performance of SAE-Scaling, with results presented in Figure 4. The analysis reveals two dis-
 429 tinct phases: (1) For the first seven turns, accuracy shows a clear upward trend, with SAE-Scaling
 430 consistently outperforming the Budget Forcing baseline. Consistent with our main experiments, this
 431 demonstrates that by actively controlling the LLM’s reasoning strategy, our method generates more

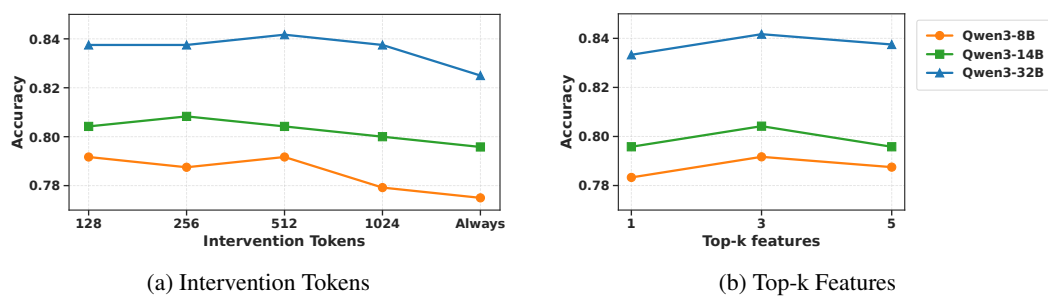


Figure 5: Sensitivity analysis of critical hyperparameters with experiments conducted on AIME24.

productive reasoning trajectories with the same test time computation. (2) After the seventh turn, performance becomes unstable and declines, with accuracy after 14 turns falling even below the initial accuracy. This suggests that reasoning trajectories should not be excessively extended.

To understand the cause of this decline, we tracked the number of problems switching from incorrect to correct (corrections) versus correct to incorrect (regressions) at each turn, as depicted in Figure 4c. During the initial seven turns, corrections increase rapidly before reaching a steady state, while regressions remain negligible. Beyond this point, however, regressions begin to surge, eventually offsetting the gains from corrections and causing the overall accuracy to drop. This suggests that excessively forcing the continuation of CoT by inserting “wait” tokens may cause the LLM to lose conviction in its correct answers, making it prone to harmful revisions.

Impact of Intervention Tokens. To assess how the choice of intervention tokens affects reasoning performance, we conduct a series of experiments by varying the number of intervention tokens. As shown in Figure 5a, when the number of intervention tokens ranges from 128 to 512, there is no significant difference in performance. It is plausible that intervening on the first 128 tokens is already sufficient to adjust the reasoning strategy of the LLM, thereby guiding it toward the desired reasoning strategy. However, when the number of intervention tokens is increased to 1024 or when intervention is applied throughout the entire generation process, performance instead drops. By examining the generated responses, we observed that excessive intervention often led to repetitive output (Fu et al., 2021), which in turn reduced performance.

Impact of Top- k Features Selection. The final stage of our feature pipeline is parameterized by Top- k , which specifies the number of top steering-capable features retained for each reasoning strategy. We assess our method’s sensitivity to this hyperparameter by varying k and measuring the resulting downstream reasoning performance. As shown in Figure 5b, performance peaks at $k=3$. A smaller k (e.g., $k=1$) yields suboptimal results, likely because the single best-performing feature on the training set may not generalize optimally to the test set, whereas a slightly larger k improves feature coverage and robustness. Conversely, a larger k (e.g., $k=5$) also degrades performance, as the oversized candidate pool can introduce noise and increase the difficulty for the router to identify appropriate features.

5 CONCLUSION.

In this work, we propose to actively guide the LLM’s reasoning trajectory during TTS, thereby channeling additional computation towards more productive reasoning. To achieve this, we propose SAE-Scaling, a controllable TTS framework, which steers LLMs’ reasoning strategies by manipulating strategy-specific features identified via SAE. A lightweight strategy router dynamically determines the effective strategy for the different reasoning context, ensuring adaptive and effective guidance. Extensive experiments on three LLMs of varying scales across three challenging reasoning benchmarks demonstrate the effectiveness and robustness of SAE-Scaling, highlighting the significance of steering LLM’s reasoning trajectory during TTS. Due to limited space, we refer to Appendix B for limitation and future work.

486 REPRODUCIBILITY STATEMENT.
487488 To ensure the reproducibility of our work, we have taken the following steps. First, our study is
489 based exclusively on publicly available datasets. Second, we provide comprehensive details of our
490 methodology—including SAE training protocols, hyperparameters, and experimental settings—in
491 Section 4.1 and Appendix D. Third, we commit to releasing the complete source code, data, trained
492 SAE models, and strategy-specific features to the public after the peer-review process.
493494 REFERENCES
495496 AIME. Aime problems and solutions, 2025. URL [https://artofproblemsolving.com/
497 wiki/index.php/AIME_Problems_and_Solutions](https://artofproblemsolving.com/wiki/index.php/AIME_Problems_and_Solutions).498 Mislav Balunović, Jasper Dekoninck, Ivo Petrov, Nikola Jovanović, and Martin Vechev. Math-
499 arena: Evaluating llms on uncontaminated math competitions, February 2025. URL <https://matharena.ai/>.
500501 Trenton Bricken, Adly Templeton, Joshua Batson, Brian Chen, Adam Jermyn, Tom Con-
502 erly, Nick Turner, Cem Anil, Carson Denison, Amanda Askell, Robert Lasenby, Yifan Wu,
503 Shauna Kravec, Nicholas Schiefer, Tim Maxwell, Nicholas Joseph, Zac Hatfield-Dodds, Alex
504 Tamkin, Karina Nguyen, Brayden McLean, Josiah E Burke, Tristan Hume, Shan Carter,
505 Tom Henighan, and Christopher Olah. Towards monosemanticity: Decomposing language
506 models with dictionary learning. *Transformer Circuits Thread*, 2023. [https://transformer-
508 circuits.pub/2023/monosemantic-features/index.html](https://transformer-
507 circuits.pub/2023/monosemantic-features/index.html).509 Runjin Chen, Zhenyu Zhang, Junyuan Hong, Souvik Kundu, and Zhangyang Wang. SEAL: steer-
510 able reasoning calibration of large language models for free. *arXiv preprint arXiv:2504.07986*,
511 [abs/2504.07986](https://arxiv.org/abs/2504.07986), 2025.
512513 Boyi Deng, Yu Wan, Baosong Yang, Yidan Zhang, and Fuli Feng. Unveiling language-specific fea-
514 tures in large language models via sparse autoencoders. In *ACL (1)*, pp. 4563–4608. Association
515 for Computational Linguistics, 2025.516 Nelson Elhage, Tristan Hume, Catherine Olsson, Nicholas Schiefer, Tom Henighan, Shauna Kravec,
517 Zac Hatfield-Dodds, Robert Lasenby, Dawn Drain, Carol Chen, Roger B. Grosse, Sam McCan-
518 dlish, Jared Kaplan, Dario Amodei, Martin Wattenberg, and Christopher Olah. Toy models of
519 superposition. *arXiv preprint arXiv:2209.10652*, 2022.
520521 Zihao Fu, Wai Lam, Anthony Man-Cho So, and Bei Shi. A theoretical analysis of the repetition
522 problem in text generation. In *AAAI*, 2021.523 Andrey V. Galichin, Alexey Dontsov, Polina Druzhinina, Anton Razhigaev, Oleg Y. Rogov, Elena
524 Tutubalina, and Ivan V. Oseledets. I have covered all the bases here: Interpreting reasoning
525 features in large language models via sparse autoencoders. *arXiv preprint arXiv:2503.18878*,
526 2025.
527528 Kanishk Gandhi, Ayush Chakravarthy, Anikait Singh, Nathan Lile, and Noah D. Goodman. Cog-
529 nitive behaviors that enable self-improving reasoners, or, four habits of highly effective stars.
530 *Second Conference on Language Modeling*, 2025.531 Sandeep Reddy Gantla. Exploring mechanistic interpretability in large language models: Chal-
532 lenges, approaches, and insights. In *2025 International Conference on Data Science, Agents &*
533 *Artificial Intelligence (ICDSAAI)*, 2025.
534535 Leo Gao, Tom Dupré la Tour, Henk Tillman, Gabriel Goh, Rajan Troll, Alec Radford, Ilya Sutskever,
536 Jan Leike, and Jeffrey Wu. Scaling and evaluating sparse autoencoders. In *ICLR*, 2025.
537538 Aryo Pradipta Gema, Alexander Hägele, Runjin Chen, Andy Arditi, Jacob Goldman-Wetzler, Kit
539 Fraser-Taliente, Henry Sleight, Linda Petrini, Julian Michael, Beatrice Alex, Pasquale Minervini,
Yanda Chen, Joe Benton, and Ethan Perez. Inverse scaling in test-time compute, 2025.

540 Daya Guo, Dejian Yang, Haowei Zhang, Junxiao Song, Ruoyu Zhang, Runxin Xu, Qihao Zhu,
 541 Shirong Ma, Peiyi Wang, Xiao Bi, et al. Deepseek-r1: Incentivizing reasoning capability in llms
 542 via reinforcement learning. *arXiv preprint arXiv:2501.12948*, 2025.

543

544 Robert Huben, Hoagy Cunningham, Logan Riggs Smith, Aidan Ewart, and Lee Sharkey. Sparse
 545 autoencoders find highly interpretable features in language models. In *ICLR*, 2024.

546

547 Aaron Jaech, Adam Kalai, Adam Lerer, Adam Richardson, Ahmed El-Kishky, Aiden Low, Alec
 548 Helyar, Aleksander Madry, Alex Beutel, Alex Carney, et al. Openai o1 system card. *arXiv*
 549 *preprint arXiv:2412.16720*, 2024.

550

551 Vladimir Karpukhin, Barlas Oguz, Sewon Min, Patrick Lewis, Ledell Wu, Sergey Edunov, Danqi
 552 Chen, and Wen-tau Yih. Dense passage retrieval for open-domain question answering. In *EMNLP*
 553 (1). Association for Computational Linguistics, 2020.

554

555 Aviral Kumar, Vincent Zhuang, Rishabh Agarwal, Yi Su, John D. Co-Reyes, Avi Singh, Kate
 556 Baumli, Shariq Iqbal, Colton Bishop, Rebecca Roelofs, Lei M. Zhang, Kay McKinney, Disha
 557 Shrivastava, Cosmin Paduraru, George Tucker, Doina Precup, Feryal M. P. Behbahani, and Alek-
 558 sandra Faust. Training language models to self-correct via reinforcement learning. In *ICLR*.
 559 OpenReview.net, 2025.

560

561 Jia LI, Edward Beeching, Lewis Tunstall, Ben Lipkin, Roman Soletskyi, Shengyi Costa Huang,
 562 Kashif Rasul, Longhui Yu, Albert Jiang, Ziju Shen, Zihan Qin, Bin Dong, Li Zhou, Yann
 563 Fleureau, Guillaume Lample, and Stanislas Polu. Numinamath. [<https://huggingface.co/AI-MO/NuminaMath-1.5>] (https://github.com/project-numina/aimo-progress-prize/blob/main/report/numina_dataset.pdf), 2024.

564

565 Chin-Yew Lin. ROUGE: A package for automatic evaluation of summaries. In *Text Summarization
 Branches Out*, 2004.

566

567 Aman Madaan, Niket Tandon, Prakhar Gupta, Skyler Hallinan, Luyu Gao, Sarah Wiegreffe, Uri
 568 Alon, Nouha Dziri, Shrimai Prabhumoye, Yiming Yang, Shashank Gupta, Bodhisattwa Prasad
 569 Majumder, Katherine Hermann, Sean Welleck, Amir Yazdanbakhsh, and Peter Clark. Self-refine:
 570 Iterative refinement with self-feedback. In *NeurIPS*, 2023.

571

572 Sara Vera Marjanović, Arkil Patel, Vaibhav Adlakha, Milad Aghajohari, Parishad BehnamGhader,
 573 Mehar Bhatia, Aditi Khandelwal, Austin Kraft, Benno Krojer, Xing Han Lù, Nicholas
 574 Meade, Dongchan Shin, Amirhossein Kazemnejad, Gaurav Kamath, Marius Mosbach, Karolina
 575 Stańczak, and Siva Reddy. Deepseek-r1 thoughtology: Let's think about llm reasoning. *arXiv*
 576 *preprint arXiv:2504.07128*, 2025.

577

578 Niklas Muennighoff, Zitong Yang, Weijia Shi, Xiang Lisa Li, Li Fei-Fei, Hannaneh Hajishirzi, Luke
 579 Zettlemoyer, Percy Liang, Emmanuel J. Candès, and Tatsunori Hashimoto. s1: Simple test-time
 scaling. *arXiv preprint arXiv:2501.19393*, 2025.

580

581 Neel Nanda and Joseph Bloom. Transformerlens. <https://github.com/TransformerLensOrg/TransformerLens>, 2022.

582

583 nostalgebraist. Interpreting gpt: The logit lens. *Less-Wrong (blog)*, 2020.

584

585 OpenAI. Openai o3-mini system card, February 2025. URL <https://openai.com/index/o3-mini-system-card/>. Accessed: 2025-02-21.

586

587 Qianjun Pan, Wenkai Ji, Yuyang Ding, Junsong Li, Shilian Chen, Junyi Wang, Jie Zhou, Qin Chen,
 588 Min Zhang, Yulan Wu, and Liang He. A survey of slow thinking-based reasoning llms using
 589 reinforced learning and inference-time scaling law. *arXiv preprint arXiv:2505.02665*, 2025.

590

591 Kishore Papineni, Salim Roukos, Todd Ward, and Wei-Jing Zhu. Bleu: a method for automatic
 592 evaluation of machine translation. In *ACL*, 2002.

593

Donald B Rubin. Estimating causal effects of treatments in randomized and nonrandomized studies.
Journal of educational Psychology, 1974.

594 Leheng Sheng, An Zhang, Zijian Wu, Weixiang Zhao, Changshuo Shen, Yi Zhang, Xiang Wang,
 595 and Tat-Seng Chua. On reasoning strength planning in large reasoning models. *arXiv preprint*
 596 *arXiv:2506.08390*, 2025.

597 Chandan Singh, Jeevana Priya Inala, Michel Galley, Rich Caruana, and Jianfeng Gao. Rethinking
 598 interpretability in the era of large language models. *arXiv preprint arXiv:2402.01761*, 2024.

600 Charlie Victor Snell, Jaehoon Lee, Kelvin Xu, and Aviral Kumar. Scaling LLM test-time compute
 601 optimally can be more effective than scaling parameters for reasoning. In *ICLR*. OpenReview.net,
 602 2025.

603 Chung-En Sun, Ge Yan, and Tsui-Wei Weng. Thinkedit: Interpretable weight editing to mitigate
 604 overly short thinking in reasoning models. *arXiv preprint arXiv:2503.22048*, 2025.

606 Xinyu Tang, Xiaolei Wang, Zhihao Lv, Yingqian Min, Xin Zhao, Binbin Hu, Ziqi Liu, and Zhiqiang
 607 Zhang. Unlocking general long chain-of-thought reasoning capabilities of large language mod-
 608 els via representation engineering. In *ACL (1)*, pp. 6832–6849. Association for Computational
 609 Linguistics, 2025.

610 Openthoughts Team. Openthoughts: Data recipes for reasoning models, 2025a.

611 Qwen Team. Qwen3 technical report, 2025b.

612 Aäron van den Oord, Yazhe Li, and Oriol Vinyals. Representation learning with contrastive predic-
 613 tive coding. *arXiv preprint arXiv:1807.03748*, 2018.

614 Jason Wei, Xuezhi Wang, Dale Schuurmans, Maarten Bosma, Brian Ichter, Fei Xia, Ed H. Chi,
 615 Quoc V. Le, and Denny Zhou. Chain-of-thought prompting elicits reasoning in large language
 616 models. In *NeurIPS*, 2022.

617 Tong Wu, Chong Xiang, Jiachen T. Wang, and Prateek Mittal. Effectively controlling reasoning
 618 models through thinking intervention. *arXiv preprint arXiv:2503.24370*, 2025.

619 Chenxu Yang, Qingyi Si, Mz Dai, Dingyu Yao, Mingyu Zheng, Minghui Chen, Zheng Lin, and
 620 Weiping Wang. Test-time prompt intervention, 2025a.

621 Jingyuan Yang, Rongjun Li, Weixuan Wang, Ziyu Zhou, Zhiyong Feng, and Wei Peng. Lf-steering:
 622 Latent feature activation steering for enhancing semantic consistency in large language models.
 623 *arXiv preprint arXiv:2501.11036*, 2025b.

624 Wojciech Zaremba, Evgenia Nitishinskaya, Boaz Barak, Stephanie Lin, Sam Toyer, Yaodong Yu,
 625 Rachel Dias, Eric Wallace, Kai Xiao, Johannes Heidecke, et al. Trading inference-time compute
 626 for adversarial robustness. *arXiv preprint arXiv:2501.18841*, 2025.

627 Zhiyuan Zeng, Qinyuan Cheng, Zhangyue Yin, Yunhua Zhou, and Xipeng Qiu. Revisiting the test-
 628 time scaling of o1-like models: Do they truly possess test-time scaling capabilities? In *ACL (1)*,
 629 pp. 4651–4665. Association for Computational Linguistics, 2025.

630 Qiyuan Zhang, Fuyuan Lyu, Zexu Sun, Lei Wang, Weixu Zhang, Zhihan Guo, Yufei Wang, Irwin
 631 King, Xue Liu, and Chen Ma. What, how, where, and how well? A survey on test-time scaling in
 632 large language models. *arXiv preprint arXiv:2503.24235*, 2025.

633 Lianmin Zheng, Wei-Lin Chiang, Ying Sheng, Tianle Li, Siyuan Zhuang, Zhanghao Wu, Yonghao
 634 Zhuang, Zhuohan Li, Zi Lin, Eric P. Xing, Joseph E. Gonzalez, Ion Stoica, and Hao Zhang.
 635 Lmsys-chat-1m: A large-scale real-world LLM conversation dataset. In *ICLR*. OpenReview.net,
 636 2024.

637 Qihuang Zhong, Kang Wang, Ziyang Xu, Juhua Liu, Liang Ding, and Bo Du. Achieving 97% on
 638 gsm8k: Deeply understanding the problems makes llms better solvers for math word problems.
 639 *Frontiers of Computer Science*, 2024.

640 Xudong Zhu, Jiachen Jiang, Mohammad Mahdi Khalili, and Zhihui Zhu. From emergence
 641 to control: Probing and modulating self-reflection in language models. *arXiv preprint*
 642 *arXiv:2506.12217*, abs/2506.12217, 2025.

648 A THE USE OF LARGE LANGUAGE MODELS
649650 We utilize LLMs exclusively as a writing assistant to improve the language of this manuscript.
651 Their role was strictly confined to tasks such as refining grammar, enhancing clarity, and polishing
652 prose. The LLMs are not used for any other purpose, including but not limited to research ideation,
653 methodological design, data analysis, or the interpretation of results.
654655 B LIMITATIONS AND FUTURE WORK.
656657 Despite its promising results, SAE-Scaling represents an initial attempt at controlling the reasoning
658 trajectory during TTS, leaving many future directions. First, we only explored steering five prede-
659 fined reasoning strategies. Future work could investigate steering a broader and more diverse set of
660 strategies. Second, we select the effective reasoning strategy by training a strategy router, which re-
661 quires preparing training data and incurs computational overhead. Future work could explore more
662 lightweight or data-efficient approaches for strategy selection. Third, we extend the CoT length by
663 inserting a special token at the end of the initial reasoning process. Future work could explore al-
664 ternative intervention points, such as intervening at the beginning or in the middle to dynamically
665 adjust the reasoning trajectory.
666667 C RELATED WORK
668669 **Test time scaling** refers to methods that improve LLM performance on complex reasoning tasks by
670 allocating additional computation at inference (Zhang et al., 2025). Early work has studied *parallel*
671 *scaling*, which samples multiple solution candidates in parallel and aggregates them into the final
672 answer using strategies such as best-of- N search or majority voting. More recently, the success
673 of LLMs such as GPT- $o3$ (OpenAI, 2025) and DeepSeek-R1 (Guo et al., 2025) has highlighted
674 the potential of *sequential scaling*, in which an LLM produces a long CoT such as reflection and
675 backtracking, ultimately improving reasoning performance (Marjanović et al., 2025; Madaan et al.,
676 2023). To extend a LLM’s CoT length beyond its default stopping point, current approaches typi-
677 cally insert special tokens (e.g., `wait`) when the LLM is about to conclude reasoning, forcing it to
678 continue and generate a longer CoT (Muennighoff et al., 2025). However, these approaches focus
679 mainly on prolonging the CoT while lacking mechanisms to improve the quality of the additional
680 reasoning. Consequently, the extended CoTs often include repetitive content or aimless exploration,
681 which undermines their overall effectiveness (Zeng et al., 2025; Gema et al., 2025). To address this
682 limitation, we propose SAE-Scaling, a method that guides the LLM to produce CoTs that are not
683 only longer but also towards appropriate reasoning strategy.
684685 **Thinking intervention** aims to directly influence the intermediate reasoning process of LLMs to
686 guide and control their reasoning trajectories (Wu et al., 2025). Some studies attempt to intervene
687 in the reasoning process by injecting prompts (Wu et al., 2025; Yang et al., 2025a), but these ap-
688 proaches lack direct control over the LLM’s internal dynamics and are highly sensitive to prompt
689 wording. Other work uses representation learning to identify reasoning-related directions in the ac-
690 tivation space of LLMs, intervening during reasoning by manipulating these directions (Tang et al.,
691 2025; Chen et al., 2025; Zhu et al., 2025; Sun et al., 2025). However, such methods operate at a
692 coarse granularity—for example, controlling only the overall length of the CoT—without the ca-
693 pability to perform fine-grained steering of reasoning strategies. Conversely, we leverage SAEs to
694 decompose LLM activations into human-interpretable features and identify those associated with
695 specific reasoning strategies, thereby enabling fine-grained control over the LLM’s reasoning be-
696 havior.
697698 **Mechanistic interpretability** seeks to understand the internal workings of LLMs by analyzing the
699 structure and function of their learned representations (Singh et al., 2024; Gantla, 2025). A pri-
700 mary tool in this field is SAEs, which decompose high-dimensional LLM activations into a sparse
701 set of latent features (Bricken et al., 2023; Huben et al., 2024). These features often correspond
702 to human-interpretable concepts, enabling researchers to probe and manipulate specific aspects of
703 LLM behavior (Deng et al., 2025; Yang et al., 2025b). For example, Galichin et al. (2025) leveraged
704 SAEs to identify features associated with reasoning. In their method, reasoning features are selected
705 as those that activate more strongly on reasoning-related keywords (e.g., ‘`wait`’, ‘`alternatively`’) than
706

702 on other tokens. However, this correlation-based approach tends to yield coarse associations with
 703 reasoning rather than features that enable fine-grained control over specific reasoning strategies.
 704 Instead, we identify features via their logit contributions and validate them through causal interventions,
 705 enabling more fine-grained steering.
 706

707 D ADDITIONAL IMPLEMENTATION DETAILS

709 D.1 SELECTION OF STEERING STRENGTH

711 The hyper-parameter α determines the steering strength during reasoning steering. An overly large
 712 α can cause the LLM to generate repetitive outputs, while an α that is too small may yield negligible
 713 steering effects. We thus select an α value that is as large as possible without inducing repetitive
 714 outputs. Specifically, to determine this value for each feature, we start with $\alpha = 15$ and test it on 10
 715 randomly sampled problem-answer pairs from the training data. We then decrease α in decrements
 716 of 1 until no repetition is observed across any pair. The starting value of 15 was chosen empirically,
 717 as we found that higher values frequently lead to repetitive outputs for most features.
 718

719 D.2 EXTRACTION OF STRATEGY KEYWORDS

720 To extract strategy keywords for each reasoning strategy, we first construct a corpus for each reasoning
 721 strategy by sampling the responses of the LLM to a diverse set of problems and manually
 722 identifying the segments corresponding to each reasoning strategy. From each strategy-specific corpus,
 723 we then extract the top-20 most frequent words and then perform a manual curation to select the
 724 keywords we identified as most representative of the target reasoning strategy. The final key words
 725 list are shown in Table 3.
 726

727 Reasoning Strategy	728 High-Frequency Keywords
729 Problem Understanding	problem, question, statement, reads, says
730 Procedural Planning	let, need, planning, decomposition
731 Backtracking	earlier, previous, initial, back
732 Multi-Perspective Verification	another, example, case, approach
733 Hypothesis Reasoning	maybe, perhaps, assume, suppose, if

735 Table 3: High-frequency keywords corresponding to each reasoning strategy
 736

737 D.3 DATASETS

740 **Training Data for SAE.** Consistent with prior work (Galichin et al., 2025), we train our SAEs
 741 on activations from a mixed corpus combining LMSYS-CHAT-1M (Zheng et al., 2024) and
 742 OPENTHOUGHTS-114K (Team, 2025a). The former is a large-scale, general-purpose conversa-
 743 tion dataset, while the latter provides high-quality reasoning traces generated by Deepseek-R1 (Guo
 744 et al., 2025). In total, we randomly sampled 0.5B tokens, drawn evenly from the two datasets.
 745 Specifically, since our work focuses on mathematical reasoning, we exclusively sampled data from
 746 the math domain for OPENTHOUGHTS-114K.
 747

748 **Training Data for Feature Identification.** The training data for Stage 2 and Stage 3 of
 749 our feature identification pipeline is sourced from 919 problems from past AIME competitions
 750 (1983–2023) (AIME, 2025). To validate steering effects in Stage 2, we test each candidate fea-
 751 ture on 10 randomly sampled problem-answer pairs. We extend the CoT of each pair by 512 tokens
 752 and manually annotate whether the reasoning strategy was successfully steered towards the target.
 753 This corresponds to manually labeling the outcome variables $Y_p \mid do(T = 0)$ and $Y_p \mid do(T = 1)$.
 754 The sample size of 10 problems represents a trade-off between the high cost of manual annotation
 755 and the need for reliable judgments. To rank the practical utility of steering-capable features for
 Stage 3, we randomly sample 100 problem-answer pairs where the initial answer is wrong. And we
 measure the correction rate achieved by steering with each feature.
 756

756 **Training Data for Strategy Router.** For the training of our strategy router, we use a training
 757 set composed of 919 problems from past AIME competitions (1983–2023) (AIME, 2025) and 4,000
 758 problems from the ‘aops.forum’ source of the NUMINAMATH-1.5 dataset (LI et al., 2024). For each
 759 problem, we sample eight initial responses. To empirically evaluate the effectiveness of a feature
 760 f_j on an incorrect response y_i , we apply reasoning steering with f_j to generate eight responses and
 761 measure the proportion of them that successfully correct the initial error.

762 D.4 RELIABILITY OF GPT-4O AS AN EVALUATOR

763 To evaluate the steering effectiveness, we measured steering success rate, where GPT-4o judges
 764 if the target strategy appears more frequently within the extended CoTs compared to generations
 765 without steering (the full prompt is presented in Figure 8). We also compute similarity metrics
 766 (BLEU-4 (Papineni et al., 2002) and ROUGE-L (Lin, 2004)) between steered and unsteered outputs,
 767 where lower values indicate greater changes in content. The sampling temperature is fixed to 0 for
 768 steering-effectiveness evaluation to ensure that observed differences in the outputs are attributable
 769 solely to the steering intervention.

770 To validate this approach, we conducted a human annotation study. Specifically, we randomly sam-
 771 pled 100 steered outputs (20 per strategy) alongside their unsteered baselines and tasked human
 772 annotators with the same evaluation. As shown in Table 4, we calculated the agreement rate be-
 773 tween human judgments and GPT-4o’s labels. Given an overall agreement rate of 0.82, we conclude
 774 that GPT-4o is a reliable proxy for human evaluation in this task.

777 Reasoning Strategy	778 Agreement
779 Problem Understanding	0.80
780 Procedural Planning	0.75
781 Backtracking	0.80
782 Multi-perspective Verification	0.90
783 Hypothesis Reasoning	0.85
784 Average	0.82

785 Table 4: Agreement between human annotators and GPT-4o on steering success evaluation.

786 D.5 ADDITIONAL IMPLEMENTATION DETAILS.

787 We train TopK-SAEs (Gao et al., 2025) (with $K = 50$) on three Qwen3-series LLMs (Team, 2025b)
 788 with parameter sizes of 8B, 14B, and 32B. For the hyperparameter of feature selection, we set am-
 789 plify keywords number $n = 2$, logit contribution threshold $\tau = 0.1$ and ATE threshold $\delta = 0.5$.
 790 These values were empirically chosen to strike a balance between maximizing the recall of poten-
 791 tially effective features and maintaining a concise candidate set to reduce the cost of downstream
 792 verification. For evaluation, the maximum generation length is set to 32,768 tokens for initial answer
 793 generation and 16,384 tokens for the subsequent TTS process.

794 E ADDITIONAL RESULTS

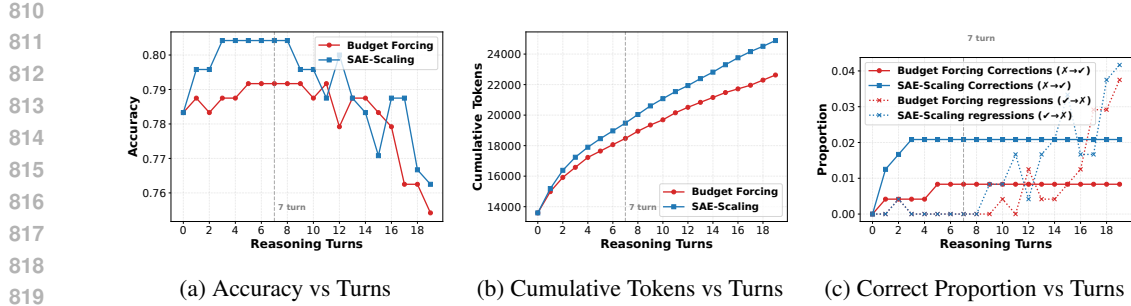


Figure 6: Impact of extended reasoning turns on performance. Results are for Qwen3-14B on AIME24.

Problem:

In triangle ABC , $AB = 10$, $BC = 14$, and $CA = 16$. Let D be a point in the interior of \overline{BC} . Let points I_B and I_C denote the incenters of triangles ABD and ACD , respectively. The circumcircles of triangles BI_BD and CI_CD meet at distinct points P and D . The maximum possible area of $\triangle BPC$ can be expressed in the form $a - b\sqrt{c}$, where a , b , and c are positive integers and c is not divisible by the square of any prime. Find $a + b + c$.

No steering extended:

Let me recall that the area of triangle ABC is $40\sqrt{3}$. If the maximum area of BPC is $40\sqrt{3} - 14\sqrt{3} = 26\sqrt{3}$, then $a = 40$, $b = 14$, $c = 3$, giving $40 + 14 + 3 = 57$. But why would the area of BPC be $26\sqrt{3}$?

...

+ Problem Understanding:

Let me think again. **The problem says** "the maximum possible area of triangle BPC can be expressed in the form $a - b\sqrt{c}$ ". Let me consider that the area might be related to the area of ABC minus some value.

...

+ Procedural Planning:

Let me check one more thing. The area of triangle BPC when P is at $(7, 7\sqrt{3})$ is $49\sqrt{3}$, but the area of triangle ABC is $40\sqrt{3}$. Since P is outside, it's possible ...

Let me try to calculate the area of BPC when P is the incenter of ABC , which is at $(4, 2\sqrt{3})$. The area is $14\sqrt{3}$, as calculated earlier. This is $14\sqrt{3}$, which is $14\sqrt{3} - 0$, but again b must be positive ...

Let me recall that in triangle BPC , with $\angle BPC = \pi/3$, and $BC = 14$...

+ Backtracking:

Actually, **let me recall that in the initial calculation**, the area of triangle ABC is $40\sqrt{3}$. If the maximum area of BPC is $40\sqrt{3}$, it would be equal to the area of ABC , but this is not possible since P is a point outside or inside.

...

+ Multi-perspective Verification:

Let me think about another approach.

Let me use the fact that the area of BPC is $(1/2) * BP * CP * \sin(\angle BPC)$, and from the earlier relation, if $\angle BPC$ is $2\pi/3$, then the maximum $BP * CP$ is $392/5$, so the area is $(392/5) * (\sqrt{3}/2) = 196\sqrt{3}/5$. But $196/5$ is 39.2 , so $39.2\sqrt{3}$ is not in the form $a - b\sqrt{c}$.

Alternatively, if the maximum area is when P is the incenter of ABC , the area is $14\sqrt{3}$, but this is also not in the required form.

Another idea: maybe the maximum area is the area of ABC , which is $40\sqrt{3}$, but the problem says "maximum possible", so it might be larger.

...

+ Hypothesis Reasoning:

Let me think again. **If** the area is $49\sqrt{3}$, and **if** the problem says it can be expressed as $a - b\sqrt{c}$, **perhaps** there is a different expression. Let me recall that $49\sqrt{3}$ is equal to $49\sqrt{3} + 0$, but if there is a different expression, like if the area is $49\sqrt{3} - \text{something}$, but I need to think.

Figure 7: A case study of reasoning steering. By steering with different strategy-specific features as control vectors, we steer the subsequent reasoning trajectory to follow different reasoning strategies.

864
 865 You are an expert AI analyst. Your task is to analyze the 'Before Intervention' and 'After Intervention' Reasoning
 866 Text below, and **for each of the five reasoning strategies**, count the number of times each strategy is present
 867 in each text, and determine whether its frequency increases after intervention.
 868
 869 Your output **MUST** be a single valid JSON object.
 870 For each strategy, provide:
 871 - "before": integer, the count of occurrences in the Before Intervention text.
 872 - "after": integer, the count of occurrences in the After Intervention text.
 873 - "more_frequent": boolean, true if the count **after** > **before**, else false.
 874
 875 The JSON object should have exactly five keys (one for each strategy), and their corresponding values should
 876 be an object as described above.
 877
 878 ---
 879 **### Strategy Definitions ###**
 880
 881 Here are the five strategies to look for:
 882
 883 1. **Procedural Planning:** The text explicitly states the next steps, defines a task, or outlines a plan. (e.g., "Let
 884 me check if ...", "I need to ...")
 885 2. **Problem Understanding:** The text involves re-stating, clarifying, or interpreting the problem statement, its
 886 constraints, or given information. (e.g., "The question says that ...", "In the problem statement, it says ...")
 887 3. **Hypothesis Reasoning:** The text makes an assumption or poses a "what if" scenario to explore possibilities
 888 or test a condition. (e.g., "If I consider that ...", "Let me assume that ...", "Suppose we had...")
 889 4. **Backtracking:** The text identifies a mistake in its own previous reasoning and attempts to correct it or go
 890 back to a previous step. (e.g., "The initial calculation is wrong ...", "Earlier, when I derived the general equation
 891 for ...", "Let me go back to the original ...")
 892 5. **Multi-perspective Verification:** The text attempts to solve the problem using a different method, checks the
 893 result with a specific example, or considers an alternative viewpoint to verify its conclusion. (e.g., "Let's try
 894 another way.", "Wait, let me check the case where ...", "Alternatively, let me check the original problem from
 895 another ...", "Another idea: ...")
 896
 897 ---
 898
 899 ****Examples:****
 900
 901 ****Input:****
 902 Before Intervention: "Let me try to verify the answer by a different method. First, I will restate the problem: the
 903 triangle has area x. If I assume a different configuration... Wait, I think I made an error earlier."
 904 After Intervention: "Let me restate the requirements: The triangle area is x, sides are y and z. I will check another
 905 approach. Suppose if the point moves, then the area changes. The previous calculation was incorrect, so let's fix
 906 it. Now I will break down the tasks: first, compute the sides, then the area."
 907
 908
 909 ****Your Answer:****
 910 `...json`
 911 `{`
 912 `"Procedural Planning": {"before": 1, "after": 2, "more_frequent": true},`
 913 `"Problem Understanding": {"before": 1, "after": 1, "more_frequent": false},`
 914 `"Hypothesis Reasoning": {"before": 1, "after": 1, "more_frequent": false},`
 915 `"Backtracking": {"before": 1, "after": 1, "more_frequent": false},`
 916 `"Multi-perspective Verification": {"before": 0, "after": 1, "more_frequent": true}}`
 917 `}`
 918
 919 ---
 920
 921 **### FINAL TASK ###**
 922
 923 ****Reasoning Texts to Analyze:****
 924
 925 Before Intervention:
 926 `@@@before_text@@@`
 927
 928 After Intervention:
 929 `@@@after_text@@@`
 930
 931 ****Your Answer:****

916
 917 Figure 8: The prompt used for evaluating steering success. We provide GPT-4o with both the
 918 steered and the unsteered outputs and ask it to determine if the target reasoning strategy appears
 919 more frequently in the steered version.

918

Algorithm 1 SAE-Scaling: Offline Feature Identification and Router Training

919

1: **Input:** Base LLM \mathcal{M} , SAE training corpus \mathcal{D}_{SAE} , feature identification corpus \mathcal{D}_{ID} , router training corpus $\mathcal{D}_{\text{Router}}$, predefined strategies $\mathcal{S} = \{s_1, \dots, s_5\}$, top-k for features k .
2: **Output:** Trained SAE, strategy-specific features $\mathcal{F}_{\text{strategy}}$, trained strategy router \mathcal{R} .

3: // Part 1: Train Sparse Autoencoder (SAE)
4: Train SAE on activations from \mathcal{D}_{SAE} to learn decoder features \mathcal{F}_{all} . {As per Sec. 3.1}
5: // Part 2: Identify Strategy-Specific Features (3-Stage Pipeline)
6: $\mathcal{F}_{\text{strategy}} \leftarrow \emptyset$
7: **for** each strategy $s \in \mathcal{S}$ **do**
8: // Stage 0: Keyword Extraction
9: $\mathcal{K}_s \leftarrow \text{ExtractKeywords}(s, \mathcal{D}_{\text{ID}})$ {Extract representative keywords for strategy s }
10: // Stage 1: Logit-based Recall
11: $\mathcal{L} \leftarrow W_{\text{dec}} \cdot U$ { W_{dec} is SAE decoder, U is LLM unembedding matrix}
12: $\mathcal{F}_{\text{candidate}} \leftarrow \text{FilterFeaturesByLogits}(\mathcal{F}_{\text{all}}, \mathcal{K}_s, \mathcal{L})$ {Select features that boost keywords' logits}
13: // Stage 2: Causal Effect Ranking
14: $\mathcal{F}_{\text{capable}} \leftarrow \emptyset$
15: **for** each feature $f \in \mathcal{F}_{\text{candidate}}$ **do**
16: $\text{ATE}(f) \leftarrow \text{EstimateCausalEffect}(f, \mathcal{D}_{\text{ID}})$ {Using Eq. 7}
17: **if** $\text{ATE}(f) \geq \delta$ **then**
18: $\mathcal{F}_{\text{capable}} \leftarrow \mathcal{F}_{\text{capable}} \cup \{f\}$
19: **end if**
20: **end for**
21: // Stage 3: Task Accuracy Ranking
22: For each $f \in \mathcal{F}_{\text{capable}}$, compute $\text{CorrectionRate}(f)$ on incorrect examples from \mathcal{D}_{ID} .
23: $\mathcal{F}_s \leftarrow \text{TopK}(\mathcal{F}_{\text{capable}}, \text{key}=\text{CorrectionRate}, k)$
24: $\mathcal{F}_{\text{strategy}} \leftarrow \mathcal{F}_{\text{strategy}} \cup \mathcal{F}_s$
25: **end for**
26: // Part 3: Train Strategy Router
27: $\mathcal{R} \leftarrow \text{TrainRouter}(\mathcal{F}_{\text{strategy}}, \mathcal{D}_{\text{Router}})$ {Using InfoNCE loss as per Eq. 9}
28: **return** SAE, $\mathcal{F}_{\text{strategy}}$, \mathcal{R}

950

Algorithm 2 SAE-Scaling: Controllable Inference

951

1: **Input:** Base LLM \mathcal{M} , a problem p , trained SAE, strategy features $\mathcal{F}_{\text{strategy}}$, router \mathcal{R} .
2: **Hyperparameters:** Steering strength α , intervention tokens N , extension turns T_{ext} .
3: **Output:** Final reasoning trajectory Y_{final} .

4: // 1. Generate initial response
5: $Y \leftarrow \text{GenerateInitialResponse}(\mathcal{M}, p)$
6: // 2. Iteratively extend the reasoning trajectory
7: **for** $t = 1$ **to** T_{ext} **do**
8: // a. Select the most effective strategy
9: $Y_{\text{context}} \leftarrow \text{GetCurrentContext}(Y)$ {e.g., the final token's hidden state}
10: $f_{\text{steer}} \leftarrow \arg \max_{f \in \mathcal{F}_{\text{strategy}}} \mathcal{R}(Y_{\text{context}}, f)$ {Use router to pick best feature}
11: // b. Steer generation for N tokens
12: $Y_{\text{extension}} \leftarrow \text{GenerateNextToken}(\mathcal{M}, Y, x'_l)$
13: **for** $i = 1$ **to** N **do**
14: Get activation x_l at the SAE-trained layer l for the current prefix Y .
15: $x'_l \leftarrow x_l + \alpha \cdot f_{\text{steer}}$ {Inject the strategy feature (Eq. 5)}
16: $y_{\text{next}} \leftarrow \text{GenerateNextToken}(\mathcal{M}, Y, x'_l)$
17: $Y \leftarrow Y + y_{\text{next}}$ {Append the new token to the full trajectory}
18: **end for**
19: **end for**
20: **return** Y
